

# A Proteomic Study Based on Home Quarantine Model Identifies NQO1 and Inflammation Pathways Involved in Adenoid Hypertrophy

Penghui Chen<sup>1-3,\*</sup>, Shule Hou<sup>1-3,\*</sup>, Xiuhong Pang<sup>4</sup>, Lei Li<sup>1-3</sup>, Wei Wei<sup>1-3</sup>

<sup>1</sup>Department of Otorhinolaryngology-Head and Neck Surgery, Xinhua Hospital, Shanghai Jiao Tong University School of Medicine, Shanghai, People's Republic of China; <sup>2</sup>Ear Institute, Shanghai Jiao Tong University School of Medicine, Shanghai, People's Republic of China; <sup>3</sup>Shanghai Key Laboratory of Translational Medicine on Ear and Nose Diseases, Shanghai Jiao Tong University School of Medicine, Shanghai, People's Republic of China; <sup>4</sup>Department of Otolaryngology-Head and Neck Surgery, the Affiliated Taizhou People's Hospital of Nanjing Medical University, Taizhou School of Clinical Medicine, Nanjing Medical University, Taizhou, Jiangsu, People's Republic of China

\*These authors contributed equally to this work

Correspondence: Wei Wei, Department of Otolaryngology-Head & Neck Surgery, Xinhua Hospital affiliated to Shanghai Jiao Tong University School of Medicine, 1665 Kongjiang Road, Yangpu District, Shanghai, 200082, People's Republic of China, Tel +86-21-25078893, Fax +86-21-65152394, Email [weiwei8319@xinhumed.com.cn](mailto:weiwei8319@xinhumed.com.cn); [xyyh2711@126.com](mailto:xyyh2711@126.com),

**Background:** Adenoid hypertrophy is a common disorder of childhood, and has an unclear pathogenesis. At the beginning of the COVID-19 pandemic, there was a significant reduction in the incidence of adenoid hypertrophy in children under long-term home quarantine, providing a rare research model to explore the pathogenesis and treatment targets of adenoidal hypertrophy in children.

**Methodology:** Before and during the home quarantine period, adenoids that underwent surgery were detected using label-free proteomics. Differences in protein expression were analyzed using Gene Ontology, the Kyoto Encyclopedia of Genes and Genomes, Gene Set Enrichment Analysis, Protein-protein interaction, and immunohistochemistry analysis.

**Results:** Long-term home quarantine had a profound impact on the proteomics of pediatric adenoids, with up-regulated and down-regulated proteins of 28 and 92 downregulated proteins, respectively. Functional enrichment analysis showed that the differentially expressed proteins were mainly enriched in pathways such as leukocyte activation, inflammatory response, IL-1 production, Th17 cell differentiation, and IL-17 signaling. In the home quarantine group, inflammation-related proteins (TNF- $\alpha$ , IL-6), CD36, and S100A2, were considerably reduced, whereas NQO1 levels increased significantly, potentially alleviating adenoid hypertrophy. NQO1, CD36, NDUFS8, and NDUFAF2 exhibited strong interactions.

**Conclusion:** This study identified some candidate differential proteins, such as NQO1, CD36, S100A2, and the inflammation pathways involved in adenoid hypertrophy in preschool children.

**Keywords:** COVID-19, home quarantine, adenoidal hypertrophy, proteomics, NQO1

## Introduction

Adenoid hypertrophy is a common disease in pediatric otolaryngology,<sup>1</sup> particularly in children aged 3–6 years, and can cause various symptoms such as nasal congestion, habitual open-mouth breathing, snoring, and obstructive sleep apnea.<sup>2</sup> In addition, it may lead to mechanical obstruction of the pharyngeal opening of the auditory tube, leading to recurrent otitis media with effusion, ultimately affecting the quality of life of children and interfering with their psychological and physiological development.<sup>3</sup>

The main causes of adenoid hypertrophy in children are recurrent respiratory infections, inflammatory stimulation of nasal sinusitis, changes in the body's immune status, and repeated irritation from allergens.<sup>4,5</sup> However, the exact key molecules and mechanisms are still unclear. Due to the lack of effective targeted drugs, adenoidectomy, nasal steroids, and anti-leukotrienes are considered the first choice for severe adenoid hypertrophy in children.<sup>6,7</sup> However, these treatments had some definite side effect. For example, a study reported that the

incidence of primary bleeding after adenoidectomy was 2.43%, with 15–25% of patients experiencing complications, including snoring, foul odor, and fever.<sup>8,9</sup>

Infection by pathogens in public places such as schools is the main cause of upper respiratory tract infections in children.<sup>10,11</sup> On January 31, 2020, COVID-19 was listed as an international public-health emergency. Because of the absence of any drug intervention, to reduce the spread of COVID-19, several countries, including China, implemented strict long-term home quarantine measures, including nationwide school closures and mask-wearing, before March 5, 2020.<sup>12,13</sup> This created a rare research model to observe how long-term home quarantine measures, including school closures, influence adenoidal hypertrophy in children. Multiple countries have reported that during the home quarantine period, the symptoms and quality of life of children with adenoid hypertrophy have significantly improved and the surgical intervention rate for pediatric adenoidal hypertrophy has significantly decreased.<sup>12,14–16</sup> Further research is needed to understand the effects of long-term home quarantine on adenoid hypertrophy.

Proteomics focuses on qualitative and quantitative analyses of all proteins in living organisms.<sup>17</sup> Label-free is a non-labeled quantitative proteomics technique that does not rely on isotope labeling.<sup>18</sup> Liquid chromatography-mass spectrometry was used to perform mass spectrometry analysis of the protein enzymatic hydrolysis peptides.<sup>19</sup> This study obtained adenoid tissues that underwent surgery before the epidemic (March 2019 to June 2019) and during the home-quarantine period (March 2020 to June 2020). Label-free comparative proteomic quantitative analysis was used to compare the differential protein expression of adenoids between the two periods, and bioinformatics research was conducted to explore the pathogenesis of adenoid hypertrophy and identify potential therapeutic targets.

# Materials and Methods

## Basic Information of Included Research Subjects

Four preschool children with adenoid hypertrophy who underwent surgical treatment at the Otolaryngology-Head and Neck Surgery Department of Xinhua Hospital Affiliated to Shanghai Jiao Tong University School of Medicine from March 2020 and June 2020 were randomly selected as the home quarantine group (HQ group), and nine preschool children with adenoid hypertrophy who underwent surgical treatment between March 2019 and June 2019 were randomly selected as the control group (control group). The general and clinical data of all children are shown in Table 1. There were no statistically significant differences in sex, age, disease course, or degree of adenoid hypertrophy between the two groups. All guardians voluntarily participated in this clinical study and signed informed consent forms after being

**Table 1** General Information and Clinical Data

	Gender	Age at Operation (month)	Duration of Snoring and Mouth Breathing (m)	A/N Ratio	BMI	Size of Tonsil Before Operation	Preoperative PSG		Extracapsular Tonsillectomy
							AHI	Lowest SaO <sub>2</sub> %	
A1	M	72	6	0.87	18.8	2+	12.5	86.5	Yes
A2	M	74	8	0.79	18.1	3+	14.6	88.8	Yes
A3	F	75	6	0.78	19.84	2+	10	83.1	Yes
A4	M	82	12	0.75	20.5	4+	15.2	82.3	Yes
C1	F	72	12	0.66	21.4	3+	11.2	87.5	Yes
C2	M	48	12	0.72	22.4	2+	13.2	86.8	Yes
C3	M	70	6	0.58	21.1	3+	13	84.1	Yes
C4	M	73	12	0.8	20.1	2+	13.3	85.3	Yes
C5	F	52	5	0.76	19.1	2+	12.2	91.1	Yes
C6	F	60	5	0.9	19.2	2+	11.5	87.9	Yes
C7	F	51	5	0.95	19.1	2+	14.6	84.6	Yes
C8	F	61	6	0.72	18.7	3+	10.6	86.1	Yes
C9	M	64	6	0.76	18.9	3+	13.2	85.3	Yes

**Abbreviations:** BMI, body mass index; PSG, polysomnography; AHI, apnea/hypopnea index; RDI, respiratory distress index.

informed of the research protocol. This prospective study was approved by the Medical Ethics Committee of Xinhua Hospital Affiliated to Shanghai Jiao Tong University School of Medicine (approval no. XHEC-NSFC-2020-045), which complies with the Declaration of Helsinki.

## Clinical Case Inclusion Criteria

Age 4–7 years old; diagnostic criteria for adenoid hypertrophy: ① Symptoms: repeated snoring with open mouth breathing during sleep; ② Signs: glandular appearance; ③ auxiliary examination: Adenoid X-ray A/N ratio, defined as the ratio of the measurement of the adenoid thickness and the nasopharyngeal aperture (the distance between the basioccipital and posterior edge of the hard palate)  $\geq 60\%$ . None of the patients had received any medication, such as montelukast, glucocorticoids, or antibiotics, in the previous week.

## Exclusion Criteria

Diseases that cause sleep-breathing disorders include nasal or oral airway stenosis, severe organ dysfunction, mental illness, systemic immune diseases, and previous adenoid surgery.

## Adenoid Sample Sampling

Cut two groups of adenoid tissue samples (2–5g) from the study subjects on the operating table, trim them into small pieces with a side length of 0.5 cm, and place them in a cryopreservation tube. They were frozen in liquid nitrogen for more than 5 min and stored in an ultra-low temperature  $-80^{\circ}\text{C}$  refrigerator. An experienced physician performed intraoperative sampling.

## Label-Free Comparative Proteomic Quantitative Analysis

Protein samples were extracted, quantified, and hydrolyzed according to the manufacturer's protocol. LC-MS/MS analysis was performed on a Q Exactive mass spectrometer (Thermo Scientific). The peptides were loaded onto a reverse-phase trap column (Acclaim PepMap100, Thermo Scientific) connected to a C18-reversed phase analytical column (Easy Column, Thermo Scientific) in buffer A (0.1% formic acid) and separated using a linear gradient of buffer B (84% acetonitrile and 0.1% formic acid). The MS data were acquired using data-dependent dynamic selection of the most abundant precursor ions from the survey scan (300–1800m/z) for HCD fragmentation. Survey scans were acquired at a resolution of 70,000 at 200m/z the resolution for the HCD spectra was set to 17,500 at 200m/z, and the isolation width was 2m/z. The normalized collision energy was 30 eV and the underfill ratio, which specified the minimum percentage of the target value likely to be reached at the maximum fill time, was defined as 0.1%.

The protein sequence database (Swissprot\_Homo\_sapiens\_20395) was downloaded from UniProt, and this database and its reverse decoy were searched using the MaxQuant software. Trypsin was set as a specific enzyme with up to 2 miss cleavage; oxidation[M] was considered a variable modification, and carbamidomethyl[C] was set as a fixed modification; false discovery rate (FDR) thresholds for proteins, peptides, and modification sites were specified at 1%. Razors and other unique peptides were used for the protein quantification. Proteins were quantified using normalized summed peptide intensity. A fold change  $\geq 2$  ( $p < 0.05$ ) was used as the threshold to define significantly changed proteins.

## Gene Ontology (GO) and KEGG Enrichment Analysis

The sequences of the selected differentially expressed proteins were locally searched using NCBI BLAST+ client software and InterProScan to find homolog sequences, gene ontology (GO) terms were mapped, and sequences were annotated using the software program Blast2GO. GO annotation results were plotted using R scripts. The studied proteins were blasted against the online Kyoto Encyclopedia of Genes and Genomes (KEGG) database (<http://geneontology.org/>) to retrieve their KEGG orthologs, which were subsequently mapped to KEGG pathways.

Enrichment analysis was performed using Fisher's exact test, with all quantified proteins considered as the background dataset. The Benjamini-Hochberg correction for multiple testing was further applied to adjust the derived p-values. Only functional categories and pathways with p-values below a threshold of 0.05, were considered significant.

## Protein-Protein Interaction (PPI)

The protein-protein interaction (PPI) information of the proteins was significantly differentially expressed in the HQ group relative to the control group retrieved from the IntAct molecular interaction database (<http://www.ebi.ac.uk/intact/>) using their gene symbols or STRING software (<http://string-db.org/>). The results were downloaded in XGMML format and imported into the Cytoscape software (<http://www.cytoscape.org/>, version 3.2.1) to visualize and analyze functional protein-protein interaction networks. Furthermore, the degree of each protein was calculated to evaluate its importance in the PPI network (score $\geq$ 0.7).

## Gene Set Enrichment Analysis (GSEA)

GSEA allows the detection of modest but coordinated changes in the expression of protein-encoding genes involved in common biological functions. GSEA was performed using R package clusterProfiler (version 3.4.1). The t-statistic mean of the genes was computed for each KEGG pathway using a permutation test with 1000 replications. Upregulated pathways were defined by a normalized enrichment score of  $>0$ . Gene sets with a P-value less than 0.05, were considered to be significantly enriched or depleted.

## Immunohistochemistry Analysis

Adenoid specimens were rinsed with PBS, dehydrated using an alcohol gradient, and embedded in paraffin sections.<sup>20</sup> The deparaffinized sections were treated with 3% H<sub>2</sub>O<sub>2</sub> and washed after antigen retrieval. They were then incubated in blocking buffer containing 5% BSA and 0.3% Triton X-100 (Sigma) for 1 h at room temperature. The following primary antibodies were used: anti-CD36 antibody (1:300; Servicebio, GB112562), anti-S100A2 antibody (1:200; Servicebio, GB111077), anti-TNF- $\alpha$  antibody (1:200; Servicebio, GB310031), anti-IL6 (1:200; Servicebio, GB12115-100), or anti-NQO1 (1:200; Abcam, ab28947) at 4°C overnight, washed three times with PBS for 10 minutes and then incubated with an HRP-secondary antibody (goat anti-rabbit and goat anti-mouse 1:300) at room temperature for 40 min. Fresh DAB chromogenic reagent was added and incubated for 10 min. Nuclei were stained with hematoxylin.

Under an Olympus optical microscope, cells with brownish-yellow particles appearing in the cytoplasm and/or cell membrane were recognized as positive. The semi-quantitative integration method was used for the analysis based on the stain score. Five 200fold field view with 200 cells counted in each field were selected. Stain score = color rendering index  $\times$  positive cell proportion index. The color rendering level was divided into four indices: 0, negative staining; 1, weak positive staining, 2=medium positive staining; and 3, strong positive staining. The positive cell proportion index was divided into five, with 0=negative, 1=positive cells accounting for 1–25%, 2=positive cells accounting for 26–50%, 3=positive cells accounting for 51–75%, and 4=positive cells accounting for 76–100%.

## Statistical Analysis

The experimental data were analyzed using SPSS statistics v19.3 software. Quantitative data were expressed as mean  $\pm$  standard deviation, and the expression levels between the two groups were compared using Wilcoxon signed-rank analysis.

## Results

### Label-Free Mass Spectrometry Data Analysis

The numbers of matched spectra, unique peptide segments, and proteins obtained in the HQ and control groups were 214319, 41258, and 5913, respectively (Figure 1A). A Venn diagram of the inter-group samples is shown in Figure 1B, which shows a remarkably identified protein overlap between the two groups. The Venn diagram in Figure 1C and D shows a remarkable overlap of protein sets identified by all biological replicates within one group. The number of upregulated and downregulated proteins and the total protein numbers were 28, 92, and 120, respectively, based on the criteria of Fold Change (FC) $>$ 2.0-fold and P-value  $<$ 0.05, respectively (*t*-test).

Cluster heat map analysis was used to compare the upregulated and downregulated differential protein expression levels between groups (Figure 1E). Hierarchical cluster analysis showed that the significantly differentially expressed



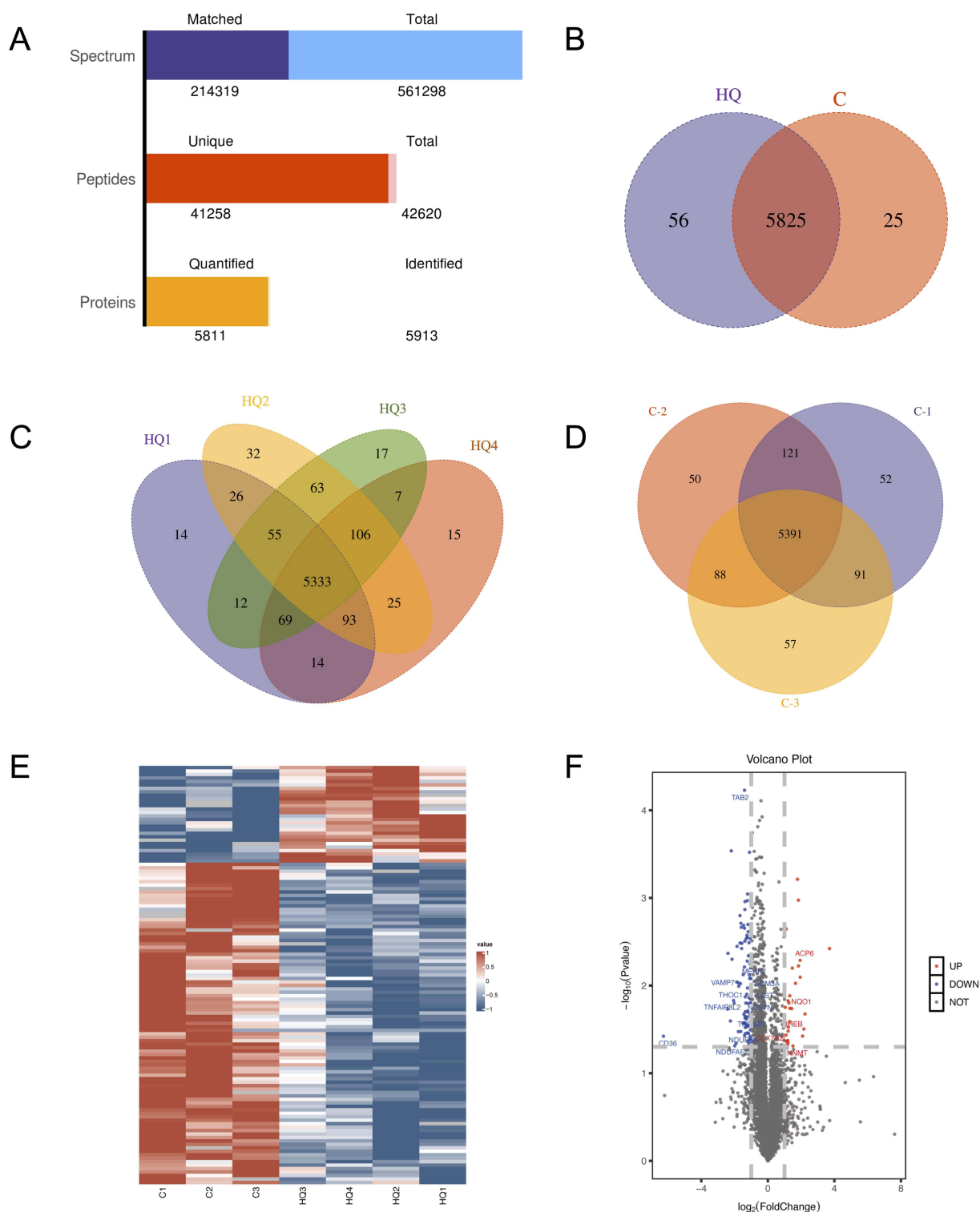


**Figure 1** Histogram, Venn diagrams, heatmap and volcano diagram of Label free mass spectrometry data. **(A)** The Histogram of the number of total and matched spectrum, unique and total peptide segments, and quantified and identified proteins obtained in this project. **(B)** Venn plots of proteins identified between the two groups. **(C)** Venn plots of all duplicated identified proteins within the HQ group. **(D)** Venn plots of all duplicated identified proteins within control group. **(E)** Hierarchically clustered heatmap of the 92 significantly deregulated proteins and 28 significantly upregulated proteins between HQ group and control group. Red represents a high z-score, and blue represents a low z-score. Hierarchical cluster analysis shows the significantly differential expressed proteins obtained can effectively distinguish these two groups, indicating that strict long-term home quarantine measures had a profound impact on the proteomics of adenoids in children ( $FC < 0.5$  and  $P < 0.05$ ,  $T$ -test). **(F)** Volcano diagram of differential expressed proteins between HQ group and control group. In volcano diagram, significantly downregulated proteins are highlighted in blue, significantly upregulated proteins are marked in red, while proteins with no difference are marked in gray ( $FC < 0.5$  and  $P < 0.05$ ,  $T$ -test).

proteins could effectively distinguish between these two groups, indicating that long-term home quarantine measures had a profound impact on the proteomics of adenoids in children. A volcanic map was drawn based on the results of the protein difference analysis of the HQ and control groups (Figure 1F). Differential analysis was conducted on 92 significantly downregulated proteins, and it was found that these proteins contained inflammatory response-related components, such as platelet glycoprotein 4 (CD36), Interleukin-6 receptor subunit beta (IL6ST), Tumor Necrosis factor alpha-induced protein 3 (TNFAIP3), and Tumor Necrosis factor-alpha-induced protein 8-like protein 2 (TNFAIP8L2). Immune-related molecules such as THO complex subunit 1 (THOC1), Alpha-1-acid glycoprotein 1, and Component C8 gamma chain. Molecule-related oxidative: NADH dehydrogenase [ubiquinone] iron-sulfur protein 8, mitochondrial (NDUFS8), NAD(P)H dehydrogenase [quinone] 1 (NQO1), Metallothionein-3 (MT3).

## Functional Enrichment Analysis

GO functional enrichment analysis of differentially expressed proteins was performed using bubble charts to display the enrichment of GO entries under the three major GO categories, as shown in Figure 2. In this comparative group, important biological processes, such as acute-phase response, regulation of interleukin-1 beta secretion, and interleukin-1 production, as well as molecular functions, such as endoplasmic reticulum, vacuolar membrane, and interleukin-6 receptor complex, were identified. Significant changes were observed in protein localization, including ion transmembrane transporter activity, endopeptidase regulator activity, and interleukin-11 binding. In GO term analysis corresponding to the deregulated proteins, cell activation, leukocyte activation, inflammatory response, platelet degranulation, acute inflammatory response, and interleukin-1 production were the top six important biological processes, as displayed in Figure 2E-F.

As shown in Figure 3, KEGG pathway enrichment analysis of differentially expressed proteins revealed significant changes in important pathways, such as oxidative phosphorylation, leukocyte transendothelial migration, oxytocin signaling, AMPK signaling, and apelin signaling. KEGG pathway enrichment analysis was performed on differentially expressed proteins, which were upregulated and downregulated and are presented in butterfly diagram form, as shown in Figure 3. KEGG pathway enrichment analysis of downregulated proteins showed changes in the valine, leucine, and isoleucine biosynthesis pathways, Th17 cell differentiation, and IL-17 signaling pathway. Enrichment and functional analyses also support the idea that the immune response, inflammatory response, and oxidative stress play key roles in the pathogenesis of adenoid hypertrophy.

## Differential Protein Analysis and Immunohistochemistry Analysis

GSEA was used to identify pathways in which the expression of genes involved in a common biological function in the HQ group was compared to the control group.<sup>21</sup> As shown in Figure 4A-D & S1, GSEA supports that the pathways, including immunity process, response to external stimulus, and antigen presentation, were deregulated, and mitochondrial activity increased in the HQ group. KEGG analysis showed that the immune process and JAK STAT signaling pathway were downregulated, whereas fatty acid metabolism and cytochrome P450 were upregulated.

To understand the exact factors involved in the pathogenesis of adenoid hypertrophy, we reanalyzed the differentially expressed proteins involved in the immune system process, response to oxidative stress, and inflammatory response. The cluster heat map is shown in Figure 4E. The differential analysis bar chart in Figure 4F-N showed that CD36, S100A2, TNFAIP8L2, IL6ST, NDUFS8, NCSTIN, VAMP7, and THOC1 were significantly higher in the control group than in the HQ group, whereas the antioxidant NQO1 experimental group was significantly higher than the control group.

In the PPI network, highly aggregated proteins often had the same or similar functions and exerted biological functions through synergistic effects, which were divided into different clusters (Figure 4O). The functional classification diagram is based on the interaction network diagram of the HQ group versus the control group. As shown in Figure 4O, the PPI network revealed strong interactions between CD36, NQO1, NDUFS8, and NDUFAF2.

Immunohistochemical analysis was used to detect CD36, S100A2, TNF- $\alpha$ , IL-6, and NQO1 protein expression in the adenoid tissues of children. Immunohistochemical analysis showed that CD36, S100A2, TNF- $\alpha$ , and IL-6 protein expression decreased in the HQ group, and NQO1 protein expression increased in the HQ group, consistent with the proteomics results, as shown in Figure 5.

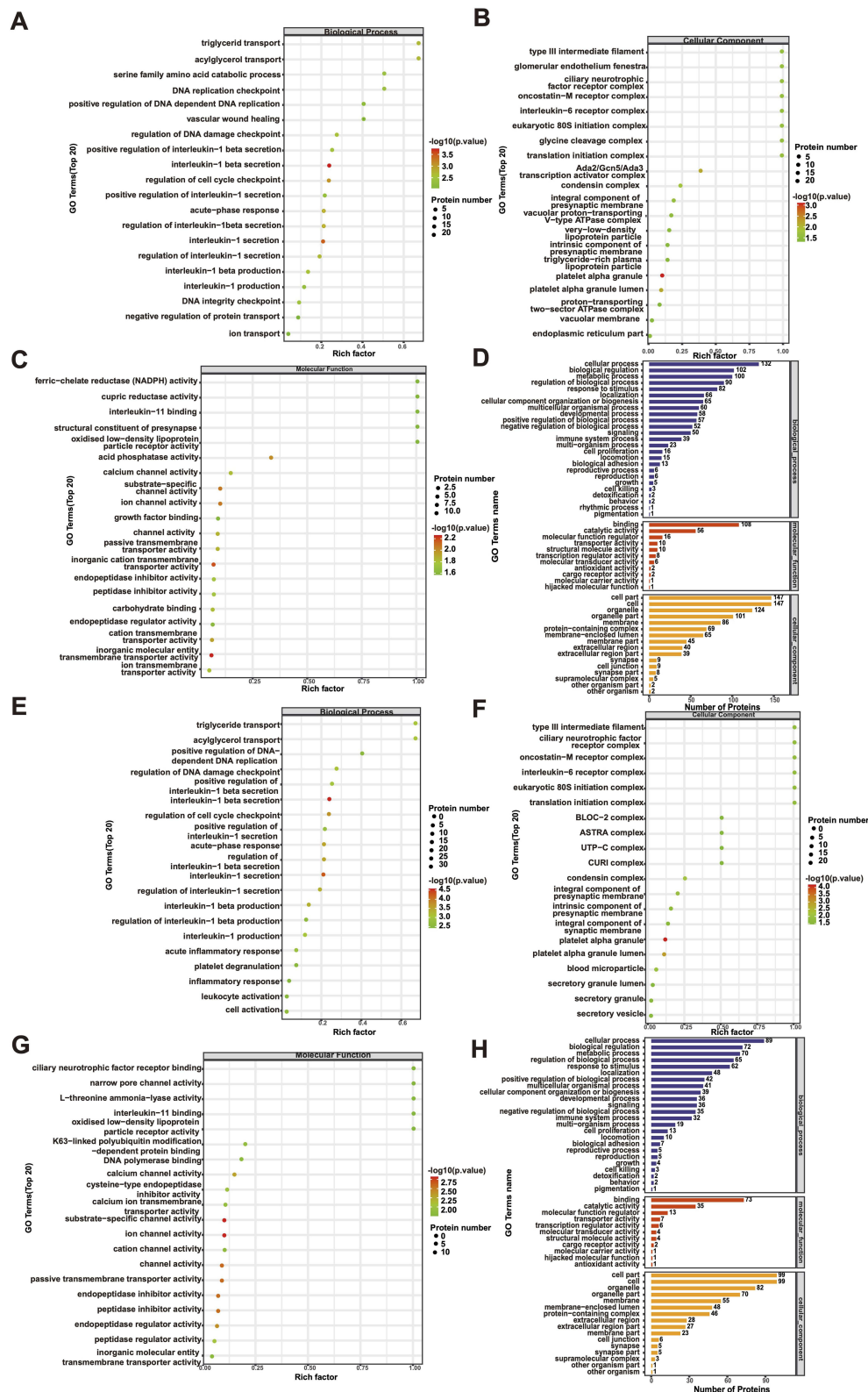


**Figure 2** The GO terms analysis of differentially expressed proteins between HQ group and control group. The bubble chart depicts the top 20 enriched GO terms (A), biological processes (B), cellular components (C), and molecular functions. GO annotation statistics for differentially expressed proteins (D). The color of each dot denotes the P value, and the size of each dot denotes the number of proteins involved in each pathway. The bubble chart depicts the top 20 enriched GO terms corresponding to deregulated proteins in biological processes (E), cellular components (F), and molecular functions (G). GO annotation statistics for differentially expressed proteins (H). The color of each dot denotes the P value, and the size of each dot denotes the number of proteins involved in each pathway.

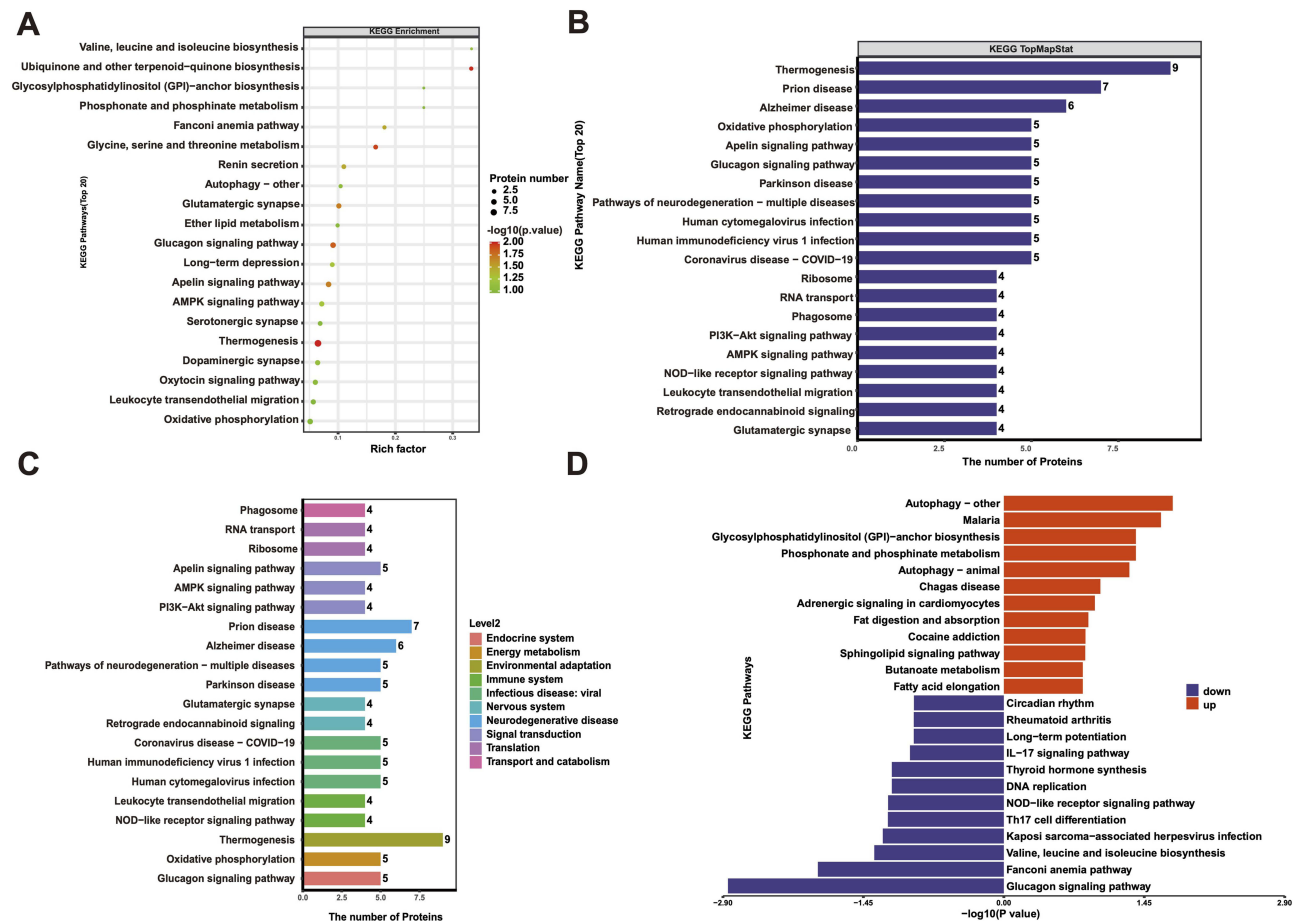


**Figure 3** KEGG pathway analysis of differentially expressed proteins between HQ group and control group. (A) The Top 20 KEGG pathway annotation statistics of differentially expressed proteins between HQ group and control group. (B) The Top 20 KEGG pathway annotation and attribution bar chart of differentially expressed proteins between HQ group and control group. (C) The Top 20 bubble diagram of KEGG pathway enrichment between HQ group and control group. (D) Enrichment butterfly diagram of pathways for upregulation and downregulation of differentially expressed proteins.

## Discussion

Adenoid hypertrophy is a common disorder of childhood, and the complex pathogenesis has not been fully studied.<sup>7</sup> Despite definitive treatment with adenoidectomy, adenoid tissue may grow after infections or chronic allergic reactions, and owing to its complications (hemorrhage, infections, emotional stress families, and the risks of general anesthesia), alternative treatments including nasal/systemic steroids, anti-histamines and anti-leukotrienes, have emerged over time.<sup>1</sup> The effectiveness of intranasal steroids or oral montelukast has been investigated.<sup>22</sup> Aleksander observed that the combined therapy was effective and reported that surgery might be replaced by anti-inflammatory therapy in patients with mild obstructive sleep apnea (OSAS).<sup>23</sup> However, steroids or montelukast have side effects, including affecting children's height development and emotional fluctuations. Physicians and parents should carefully weigh the benefits and risks of adenotonsillectomy against intranasal steroids or oral montelukast in these children.<sup>24</sup> At the beginning of the COVID-19 pandemic, the incidence rate of adenoidal hypertrophy in children was significantly reduced under long-term home quarantine measures, which provided a rare research model to explore the pathogenesis of adenoidal hypertrophy in children and drug treatment targets.<sup>12,14–16</sup> Here, we identified and analyzed the differential proteins of adenoids during the home quarantine period and before the COVID-19 epidemic using label-free mass spectrometry. The data showed that there were significant changes in the protein levels in the adenoid tissue before and after home quarantine. Significantly decreased proteins were associated with infection and allergic factors, whereas significantly increased proteins suggested the promoting effect of other pathogenic factors on adenoid hypertrophy.

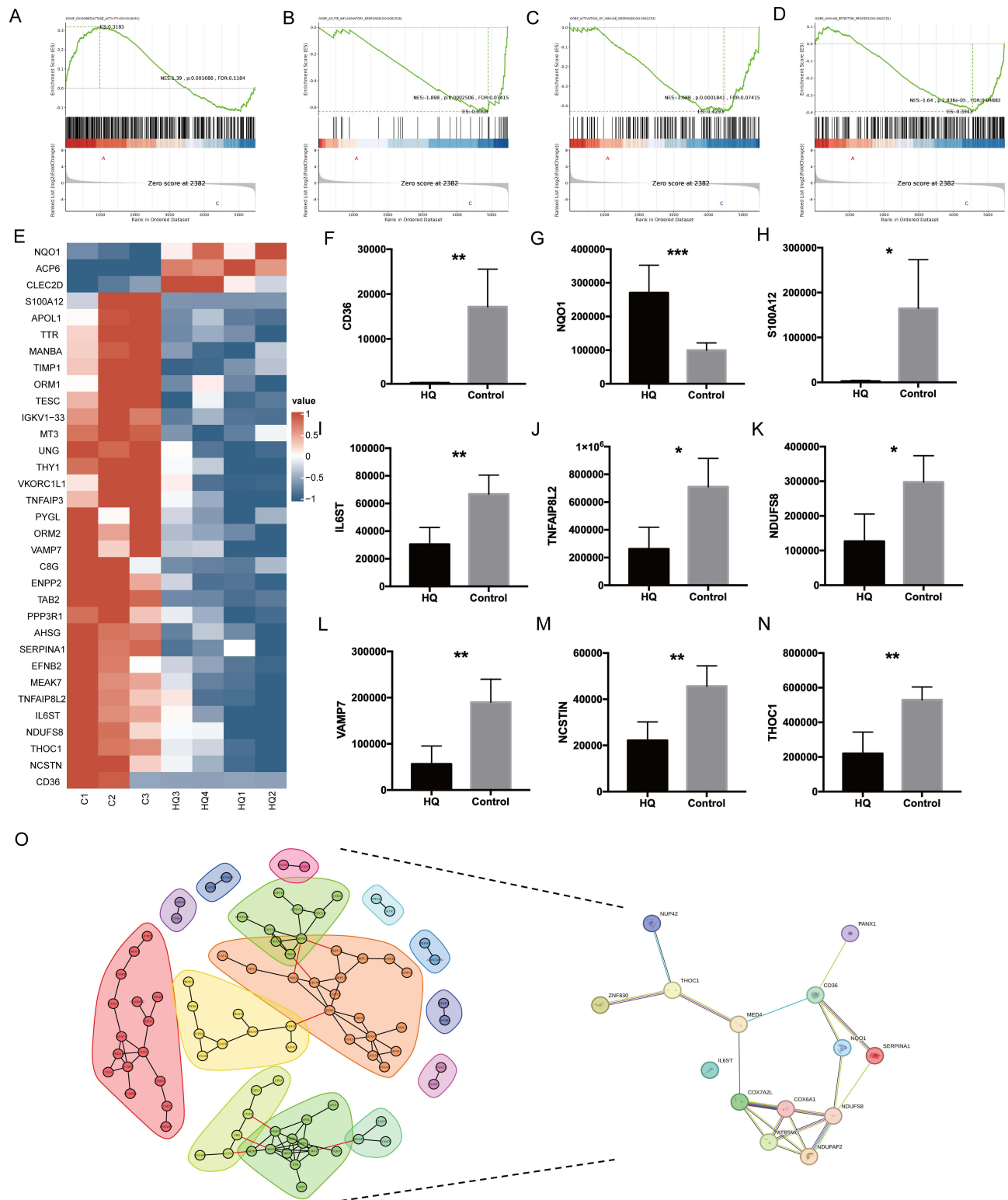


**Figure 4** GSEA, Histogram of protein expression differences and PPI of the proteomic dataset in HQ group compared to control group. GSEA demonstrated that the GO term gene sets involved oxidoreductase activity (A), acute inflammatory response (B), activation of immune response (C), and immune effector processes (D). The normalized enrichment scores (ES) and p-values are shown. The top portion of the plot shows the running ES. The middle portion of the plot shows where the members of the gene set appear in the ranked list of genes. The ranking metric measures the correlation between a gene and a phenotype. (E) Hierarchically clustered heat map of the differentially expressed proteins involved in immune system processes, oxidative stress, and inflammatory responses. (F-N) Histogram of expression differences of CD36, NQO1, S100A12, IL6ST, TNFAIP8L2, NDUFS8, VAMP7, NCSTIN, and THOC1 targeted proteins in adenoid tissue between the HQ and control groups by proteomic analysis. \* $P < 0.05$ , \*\* $P < 0.01$  and \*\*\* $P = 0.001$  compared with controls. Data are presented as the mean  $\pm$  SD,  $n \geq 3$ . (O) Functional classification based on the interaction network diagram of the HQ group vs the control group. PPI network between CD36, NQO1, NDUFS8, NDUFAF2, IL6ST, THOC1, NUP42, and SERPINA1.



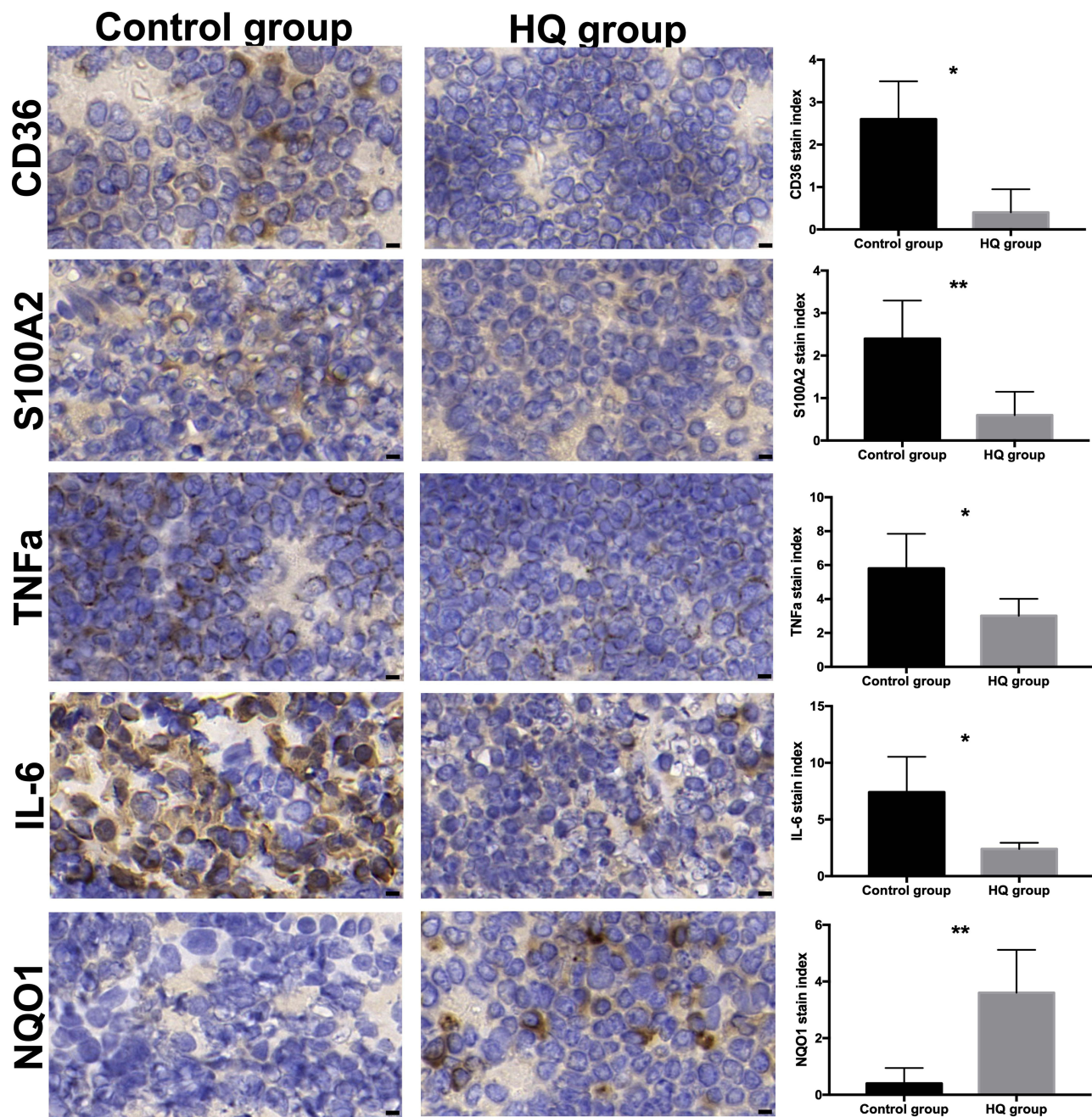


**Figure 5** The expression of CD36, S100A2, TNF- $\alpha$ , IL-6, and NQO1 in adenoid tissue between HQ group and control group by immunohistochemistry analysis. The left panel shows representative images of five target proteins in each group. The right panel shows the expression intensities of the five target proteins and the expression differences between the HQ and control groups according to the semi-quantitative integration method for immunohistochemical results. Data are presented as mean  $\pm$  SD, n= 3. \*P < 0.05 and \*\*P < 0.01 compared with controls using Wilcoxon Signed Ranks analysis. Scale bar =5  $\mu$ m.

Most researchers believe that chronic inflammatory reactions, including infections and allergic reactions, are the main causes of adenoid hypertrophy.<sup>25</sup> Long-term home quarantine, including school closure and wearing masks, helps children stay away from most infectious pathogens and allergens, reduces the occurrence of respiratory infections and allergic diseases, have a significant intervention effect on both factors.<sup>13,26</sup> Our data showed that leukocyte activation, inflammatory response, acute inflammatory response, and interleukin-1 production were downregulated after long-term home quarantine. GSEA also suggested that the acute inflammatory response, activation of immune response, immune effector process were the main downregulated pathways, while oxidoreductase activity is significantly up-regulated.

Th17 cell differentiation and IL-17 signaling pathways were downregulated in the HQ group, as shown by the KEGG analysis. According to the literature, Th17 cells can aggravate upper respiratory tract reactions by secreting IL-17.<sup>27</sup> An imbalance in Th1/Th2 and Th17/Treg cell ratios is involved in the pathogenesis of adenoid hypertrophy and is related to the degree of adenoid hypertrophy.<sup>28</sup> TNF- $\alpha$  and IL-6 are cytokines secreted by T cells and macrophages and have both pro-inflammatory and anti-inflammatory effects. Studies have shown a clear correlation between high levels of IL-6 expression in adenoid tissue and the severity of adenoid hypertrophy, and are closely related to various complications caused by adenoid hypertrophy.<sup>29</sup> Researchers have found that when adenoids are stimulated by pathogenic microorganisms, they release various inflammatory mediators including TNF- $\alpha$  and IL-6 by stimulating lymphocytes.<sup>30</sup> We speculate that TNF- $\alpha$  and IL-6 act on inflammatory cells through a certain signal transduction pathway, causing them to synthesize and release various inflammatory factors.<sup>30,31</sup> Simultaneously, they enhance the aggregation and activation ability of inflammatory cells, accelerating the vicious cycle of cytokines and inflammatory cells, leading to pathological hypertrophy of adenoids.<sup>29,32</sup> Therefore, early, active, and effective treatment of upper respiratory tract infections and allergic diseases is important for preventing and treating adenoid hypertrophy in children. TNF- $\alpha$  and IL-6, as critical inflammation factors, are potential drug targets for treating adenoid hypertrophy.

Proteomics and immunohistochemical detection showed that CD36 and S100A2 protein expression decreased in the HQ group. CD36 is the fourth major glycoprotein of the platelet surface and serves as a receptor for thrombospondin in platelets and various cell lines.<sup>33,34</sup> Abnormal CD36 overexpression promotes lipid accumulation, foam cell formation, inflammation, and thrombosis.<sup>35</sup> Many natural products target the inhibition of CD36 to prevent and treat atherosclerosis.<sup>35</sup> S100A2 is a member of the S100 protein family and contains two EF-hand calcium-binding motifs.<sup>36</sup> S100 proteins are involved in the regulation of several cellular processes such as cell cycle progression and differentiation.<sup>37</sup> S100A2 is highly upregulated in the epidermis of inflammatory skin diseases such as atopic dermatitis and psoriasis.<sup>36</sup> This study showed that because of the continuous stimulation of various microorganisms or antigens, CD36 and S100A2 were highly expressed in adenoid hypertrophy in the control group. When long-term home quarantine helps adenoids avoid microorganisms and antigens, CD36 and S100A2 are significantly down-regulated. We speculate that the abnormal overexpression of CD36 and S100A2 may also promote adenoid pathological hypertrophy, and inhibiting the upregulation of CD36 and S100A2 may prevent and treat adenoid pathological hypertrophy.

During the quarantine period, infection and allergic factors were significantly reduced through the intervention and related proteins were simultaneously downregulated. Simultaneously, the significantly upregulated proteins in surgical specimens of children with severe adenoid hypertrophy may play an important role in compensating for the etiology except infection or allergy, which may promote the effects of other pathogenic factors on adenoid hypertrophy. Both proteomic and immunohistochemical data showed that NQO1 protein expression was increased in the HQ group. The PPI network showed strong interactions between NQO1, CD36, and NDUFS8 (Figure 4). NQO1 is a member of the NAD(P)H dehydrogenase (quinone) family and encodes cytoplasmic 2-electron reductase.<sup>38</sup> It is a protective antioxidant agent, a versatile cytoprotective agent and regulates the oxidative stresses of chromatin-binding proteins for DNA damage in cancer cells.<sup>39</sup> Oxidization of cellular pyridine nucleotides causes structural alterations in NQO1 and changes its capacity to bind proteins.<sup>40</sup> Mutations in this gene have been associated with tardive dyskinesia (TD), increased risk of hepatotoxicity after exposure to benzene, and susceptibility to various forms of cancer.<sup>41,42</sup> A strategy based on NQO1 to exert a protective effect against cancer was developed using organic components to enhance NQO1 expression.<sup>40</sup> Although the above functional analysis and previous literature lack records on the correlation between NQO1 and lymphoid tissue proliferation, the results of this study suggest that overexpression or abnormal activation of NQO1 is important for adenoid hypertrophy in children.

Based on an unprecedented long-term home quarantine model, our Label-free proteomics study identified some candidate differential proteins, such as NQO1, CD36, S100A2, and inflammation pathways involved in adenoid hypertrophy in preschool children. Considering the samples of this study were screened out from a large-scale intervened population, they were relatively limited but valuable, and it would be more reliable to form a multicenter study. Further research is needed to explore the potential of these candidate proteins as therapeutic targets.

## Data Sharing Statement

The data are available from the corresponding author on reasonable request.

## Ethic Requirements

This study complies with the Declaration of Helsinki.

## Acknowledgments

Thanks to the National Science Foundation of China and the Shanghai Sailing Program for funding this work.

## Funding

This work was supported by grants from the National Natural Science Foundation of China (82000989 to PHC, 82371150, 82000977 to SLH) and the Shanghai Sailing Program (20YF1428800 to PHC, 20YF1428900 to SLH).

## Disclosure

The Authors Declare No Conflict of Interest.

## References

1. Ahmad Z, Krüger K, Lautermann J, et al. Adenoid hypertrophy-diagnosis and treatment: the new S2k guideline. *Hno*. 2023;71(Suppl 1):67–72. doi:10.1007/s00106-023-01299-6
2. Niedzielski A, Chmielik LP, Mielnik-Niedzielska G, Kasprzyk A. Adenoid hypertrophy in children: a narrative review of pathogenesis and clinical relevance. *BMJ Paediatrics Open*. 2023;7(1). doi:10.1136/bmjpo-2022-001710
3. Chmielik LP, Mielnik-Niedzielska G, Kasprzyk A, Niedzielski A. A review of health-related quality of life issues in children suffering from certain key otolaryngological illnesses. *Front Pediatr*. 2022;10:1077198. doi:10.3389/fped.2022.1077198
4. Byars SG, Stearns SC, Boomsma JJ. Association of long-term risk of respiratory, allergic, and infectious diseases with removal of adenoids and tonsils in childhood. *JAMA Otolaryngol*. 2018;144(7):594–603. doi:10.1001/jamaoto.2018.0614
5. Hu L, He W, Li J, et al. The role of adenoid immune phenotype in polysensitized children with allergic rhinitis and adenoid hypertrophy. *Pediatric Allergy Immunology*. 2024;35(6):e14166. doi:10.1111/pai.14166
6. Tamir SO, Schwarz Y, Hazan I, et al. Medical treatment does not reduce surgery rates in children with adenoid hypertrophy. *Int J Pediatr Otorhinolaryngol*. 2024;176:111836. doi:10.1016/j.ijporl.2023.111836
7. Mitchell RB, Archer SM, Ishman SL, et al. Clinical practice guideline: tonsillectomy in children (Update)-executive summary. *Otolaryngol Head Neck Surg*. 2019;160(2):187–205. doi:10.1177/0194599818807917
8. Jaensch SL, Cheng AT, Waters KA. Adenotonsillectomy for obstructive sleep apnea in children. *Otolaryngol Clin North Am*. 2024;57(3):407–419. doi:10.1016/j.otc.2024.02.025
9. Al Sebeih K, Hussain J, Albatineh AN. Postoperative complications following tonsil and adenoid removal in Kuwaiti children: a retrospective study. *Ann Med Surg*. 2018;35:124–128. doi:10.1016/j.amsu.2018.09.024
10. Ljubini-Sternak S, Meštrović T. Rhinovirus-A true respiratory threat or a common inconvenience of childhood? *Viruses*. 2023;15(4). doi:10.3390/v15040825
11. Nair H, Simões EA, Rudan I, et al. Global and regional burden of hospital admissions for severe acute lower respiratory infections in young children in 2010: a systematic analysis. *Lancet*. 2013;381(9875):1380–1390. doi:10.1016/S0140-6736(12)61901-1
12. Windfuhr JP, Günster C. Impact of the COVID-pandemic on the incidence of tonsil surgery and sore throat in Germany. *Europ Archiv Oto-Rhino-Laryngol*. 2022;279(8):4157–4166. doi:10.1007/s00405-022-07308-8
13. Lin CF, Huang YH, Cheng CY, et al. Public Health Interventions for the COVID-19 pandemic reduce respiratory tract infection-related visits at pediatric emergency departments in Taiwan. *Front Public Health*. 2020;8:604089. doi:10.3389/fpubh.2020.604089
14. Gelardi M, Giancaspro R, Fiore V, Fortunato F, Cassano M. COVID-19: effects of lockdown on adenotonsillar hypertrophy and related diseases in children. *Int J Pediatr Otorhinolaryngol*. 2020;138:110284. doi:10.1016/j.ijporl.2020.110284
15. Kourelis K, Angelopoulou M, Goulioumis A, Fouzas S, Kourelis T. Surgery for adenotonsillar hypertrophy and otitis media in children is less demanded in quarantine times. *Int J Pediatr Otorhinolaryngol*. 2022;158:111169. doi:10.1016/j.ijporl.2022.111169
16. Trecca EMC, Gaffuri M, Molinari G, et al. Impact of the COVID-19 pandemic on paediatric otolaryngology: a nationwide study. *Acta Otorhinolaryngol Ital*. 2023;43(5):352–359. doi:10.14639/0392-100X-N2452
17. Wu Q, Sui X, Tian R. Advances in high-throughput proteomic analysis. *Se Pu Chin j Chromatogr*. 2021;39(2):112–117. doi:10.3724/SP.J.1123.2020.08023
18. Rozanova S, Barkovits K, Nikolov M, et al. Quantitative mass spectrometry-based proteomics: an overview. *Methods Mol Biol*. 2021;2228:85–116.
19. Ahn YH, Kim JY, Yoo JS. Quantitative mass spectrometric analysis of glycoproteins combined with enrichment methods. *Mass Spectrom Rev*. 2015;34(2):148–165.
20. Hou S, Chen J, Yang J. Autophagy precedes apoptosis during degeneration of the Kölliker's organ in the development of rat cochlea. *Eur J Histochem*. 2019;63(2). doi:10.4081/ejh.2019.3025
21. Polleys CM, Singh P, Thieu HT, et al. Rapid, high-resolution, non-destructive assessments of metabolic and morphological homogeneity uniquely identify high-grade cervical precancerous lesions. *bioRxiv*. 2024. doi:10.1101/2024.05.10.593564



22. Chohan A, Lal A, Chohan K, Chakravarti A, Gomber S. Systematic review and meta-analysis of randomized controlled trials on the role of mometasone in adenoid hypertrophy in children. *Int J Pediatr Otorhinolaryngol.* **2015**;79(10):1599–1608. doi:10.1016/j.ijporl.2015.07.009
23. Zwierz A, Domagalski K, Masna K, Burduk P. Maximal medical treatment of adenoid hypertrophy: a prospective study of preschool children. *Europ Archiv Oto-Rhino-Laryngol.* **2024**;281(5):2477–2487. doi:10.1007/s00405-024-08459-6
24. Venekamp RP, Hearne BJ, Chandrasekharan D, et al. Tonsillectomy or adenotonsillectomy versus non-surgical management for obstructive sleep-disordered breathing in children. *Cochrane Database Syst Rev.* **2015**;2015(10):Cd011165. doi:10.1002/14651858.CD011165.pub2
25. Chirakalwasan N, Ruxrungtham K. The linkage of allergic rhinitis and obstructive sleep apnea. *Asian Pac J Allergy Immunol.* **2014**;32(4):276–286.
26. Chiu NC, Chi H, Tai Y-L. Impact of wearing masks, hand hygiene, and social distancing on influenza, enterovirus, and all-cause pneumonia during the coronavirus pandemic: retrospective national epidemiological surveillance study. *J Med Int Res.* **2020**;22(8):e21257. doi:10.2196/21257
27. Yu C, Li Y, Li Y, et al. A novel mechanism for regulating lung immune homeostasis: zukamu granules alleviated acute lung injury in mice by inhibiting NLRP3 inflammasome activation and regulating Th17/Treg cytokine balance. *J Ethnopharmacol.* **2024**;324:117831. doi:10.1016/j.jep.2024.117831
28. Ni K, Zhao L, Wu J, et al. Th17/Treg balance in children with obstructive sleep apnea syndrome and the relationship with allergic rhinitis. *Int J Pediatr Otorhinolaryngol.* **2015**;79(9):1448–1454. doi:10.1016/j.ijporl.2015.06.026
29. Tiboc-Schnell CN, Filip GA, Bolboaca SD, et al. Biomarkers of pediatric obstructive sleep apnea syndrome and the assessment of quality of life before and after adenotonsillectomy. *J Physiol Pharmacol.* **2021**;72(4). doi:10.26402/jpp.2021.4.10
30. Ye C, Guo X, Wu J, et al. CCL20/CCR6 mediated macrophage activation and polarization can promote adenoid epithelial inflammation in adenoid hypertrophy. *CData J Inflamm Res.* **2022**;15:6843–6855. doi:10.2147/JIR.S390210
31. Ferreira RC, Freitag DF, Cutler AJ, et al. Functional IL6R 358Ala allele impairs classical IL-6 receptor signaling and influences risk of diverse inflammatory diseases. *PLoS Genetics.* **2013**;9(4):e1003444. doi:10.1371/journal.pgen.1003444
32. Zhang J, Sun X, Zhong L, Shen B. IL-32 exacerbates adenoid hypertrophy via activating NLRP3-mediated cell pyroptosis, which promotes inflammation. *Mol Med Rep.* **2021**;23(3). doi:10.3892/mmr.2021.11865
33. Ashaq MS, Zhang S, Xu M, Li Y, Zhao B. The regulatory role of CD36 in hematopoiesis beyond fatty acid uptake. *Life Sci.* **2024**;339:122442. doi:10.1016/j.lfs.2024.122442
34. Chen Y, Zhang J. CD36, a signaling receptor and fatty acid transporter that regulates immune cell metabolism and fate. *J. Exp. Med* **2022**;219(6):e20211314.
35. Wen SY, Zhi X, Liu HX, et al. Is the suppression of CD36 a promising way for atherosclerosis therapy? *Biochem Pharmacol.* **2024**;219:115965. doi:10.1016/j.bcp.2023.115965
36. Liang H, Li J, Zhang K. Pathogenic role of S100 proteins in psoriasis. *Front Immunol.* **2023**;14:1191645. doi:10.3389/fimmu.2023.1191645
37. Singh P, Ali SA, Kumar S, Mohanty AK. CRISPR-Cas9 based knockout of S100A8 in mammary epithelial cells enhances cell proliferation and triggers oncogenic transformation via the PI3K-Akt pathway: insights from a deep proteomic analysis. *J Proteom.* **2023**;288:104981. doi:10.1016/j.jprot.2023.104981
38. Yuhan L, Khaleghi Ghadiri M, Gorji A. Impact of NQO1 dysregulation in CNS disorders. *J Transl Med.* **2024**;22(1):4. doi:10.1186/s12967-023-04802-3
39. Tossetta G, Fantone S. The role of NQO1 in ovarian cancer. *Int J Mol Sci* **2023**;24(9):7839.
40. Preethi S, Arthiga K, Patil AB, Spandana A, Jain V. Review on NAD(P)H dehydrogenase quinone 1 (NQO1) pathway. *Molecular Biology Reports.* **2022**;49(9):8907–8924. doi:10.1007/s11033-022-07369-2
41. Zai CC, Tiwari AK, Basile V, et al. Oxidative stress in tardive dyskinesia: genetic association study and meta-analysis of NADPH quinone oxidoreductase 1 (NQO1) and Superoxide dismutase 2 (SOD2, MnSOD) genes. *Prog Neuro Psychopharmacol Biol Psychiatry.* **2010**;34(1):50–56. doi:10.1016/j.pnpbp.2009.09.020
42. Tumbath S, Jiang L, Li X, et al.  $\beta$ -Lapachone promotes the recruitment and polarization of tumor-associated neutrophils (TANs) toward an antitumor (N1) phenotype in NQO1-positive cancers. *Oncoimmunology.* **2024**;13(1):2363000. doi:10.1080/2162402X.2024.2363000